



Identification of pathogenic fungi with an optoelectronic nose

Journal:	<i>Analyst</i>
Manuscript ID:	AN-ART-11-2013-002112.R1
Article Type:	Paper
Date Submitted by the Author:	16-Jan-2014
Complete List of Authors:	Zhang, Yinan; University of Illinois at Urbana-Champaign, Chemistry Askim, Jon; University of Illinois at Urbana-Champaign, Chemistry Zhong, Wenxuan; UIUC, Orlean, Peter; UIUC, Suslick, Kenneth; University of Illinois at Urbana-Champaign, Chemistry

Title

Identification of pathogenic fungi with an optoelectronic nose

Author names

Yinan Zhang,^a Jon R. Askim,^a Wenxuan Zhong,^b Peter Orlean,^c and Kenneth S. Suslick^{*a}

^a Department of Chemistry, ^b Department of Statistics, and ^c Department of Microbiology

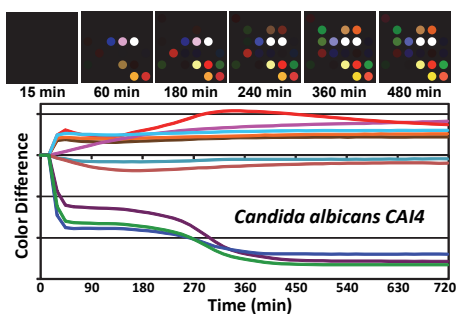
University of Illinois at Urbana-Champaign, 600 S. Mathews Av., Urbana, IL 61801, USA

Corresponding should address to * Kenneth S. Suslick E-mail: ksuslick@illinois.edu,

Department of Chemistry, University of Illinois at Urbana-Champaign, 600 S. Mathews Av.,

Urbana, IL 61801, USA.

Table of contents entry



A disposable colorimetric sensor array capable permits rapid differentiation and identification of 12 pathogenic fungi in 3 hr with >98% accuracy, based on their metabolic profiles of emitted volatiles.

Abstract

Human fungal infections have gained recent notoriety following contamination of pharmaceuticals in the compounding process. Such invasive infections are a more serious global problem, especially for immunocompromised patients. While superficial fungal infections are common and generally curable, invasive fungal infections are often life-threatening and much harder to diagnose and treat. Despite the increasing awareness of the situation's severity, currently available fungal diagnostic methods cannot always meet diagnostic needs, especially for invasive fungal infections. Volatile organic compounds produced by fungi provide an alternative diagnostic approach for identification of fungal strains. We report here an optoelectronic nose based on a disposable colorimetric sensor array capable of rapid differentiation and identification of pathogenic fungi based on their metabolic profiles of emitted volatiles. The sensor arrays were tested with 12 human pathogenic fungal strains grown on standard agar medium. Array responses were monitored with an ordinary flatbed scanner. All fungal strains gave unique composite responses within 3 hours and were correctly clustered using hierarchical cluster analysis. A standard jackknifed linear discriminant analysis gave a classification accuracy of 94% for 155 trials. Tensor discriminant analysis, which takes better advantage of the high dimensionality of the sensor array data, gave a classification accuracy of 98.1%. The sensor array is also able to observe metabolic changes in growth patterns upon the addition of fungicides, and this provides a facile screening tool for determining fungicide efficacy for various fungal strains in real time.

1. Introduction

Worldwide mortalities from human invasive fungal infections are comparable to those from tuberculosis or malaria, and mortality rates exceed 50%.¹ Fungal infections have received increasing clinical focus,²⁻⁴ and contaminated compounding pharmacies have brought this crisis to widespread public attention.^{1, 5} Despite the increasing awareness of the situation's severity, currently available fungal diagnostic methods cannot always meet diagnostic needs, especially for invasive fungal infections. Traditional culturing methods are slow and labor-intensive, immunological tests often suffer from cross contamination, and molecular diagnostic methods lack standard criteria or diagnostic scope.^{4, 6, 7} Thus, the development of new techniques for the rapid identification of fungal strains would be highly desirable.

The volatile organic compounds (VOCs) produced by fungi may have great utility as an alternative diagnostic approach. There are approximately 250 fungal VOCs identified (including alcohols, phenols, thiols, sulfides, hydrocarbons and aldehydes) that derive from fungal primary or secondary metabolic pathways.⁸ It has been shown that fungal VOC fingerprints can be used to discriminate noninvasively among medically relevant fungi⁹⁻¹¹ and to rapidly screen and monitor the effectiveness of anti-fungal drugs.^{12, 13} Previous VOC identification and profiling methods, however, are either not cost-effective or not robust. Gas chromatography-mass spectrometry (GC-MS) is high-maintenance and expensive. Moreover, sample collection methods, such as solid-phase micro-extraction (SPME), can have adsorption bias and poor recovery.⁸ Conventional electronic nose techniques, another commonly used VOC fingerprint profiling method, rely on weak and non-specific chemical interactions that induce changes in sensors' physical or electrical properties after exposure to VOCs.^{8, 14} Such electronic noses,

1
2
3 however, are generally very sensitive to changes in humidity, require frequent recalibration, and
4
5 are often limited in their sensitivity.
6
7

8
9 Previously, we have developed an optoelectronic nose approach using colorimetric sensor
10 arrays for VOC detection and identification.¹⁵⁻¹⁹ The sensor consists of a disposable array of
11 cross-responsive nanoporous pigments whose colours are changed by diverse chemical
12 interactions with analytes and which is unresponsive to changes in humidity. This portable,
13 inexpensive, and highly sensitive optoelectronic nose produces a composite response which
14 generates a unique molecular fingerprint for each analyte or mixture. Colorimetric sensor arrays
15 can differentiate and identify single analytes (e.g., toxic industrial gases^{17, 20, 21} and explosives²²)
16 at concentrations well below 1 ppm. We have also successfully demonstrated fingerprinting and
17 identification of complex odorant mixtures, including discrimination of the head gases of
18 beverages,²³⁻²⁵ the rapid identification of human pathogenic bacteria,²⁶ and even breath diagnosis
19 of lung cancer.²⁷
20
21
22
23
24
25
26
27
28
29
30
31
32
33
34
35

36 Herein, we report a colorimetric sensor array system for fungi differentiation and
37 identification by profiling the composite volatile metabolites produced during fungal growth.
38
39
40

41 **2. Experimental**

42 **2.1 VOC sensing experimental procedures**

43
44
45 12 fungal strains were tested, including *Candida albicans* (CAI-4), *Candida albicans* (B311),
46 *Candida albicans* (1-28), *Candida glabrata*-1, *Candida guilliermondii*, *Candida parapsilosis*,
47 *Trichosporon asahii* 3323, *Debaryomyces hansenii* 3333, *Candida stellatoidea*, *Candida keyfr*,
48 *Saccharomyces cerevisiae* 4742 and *Kluyveromyces lactis* (cf. Table S1) Strains were maintained
49
50
51
52
53
54
55
56
57
58
59
60

1
2
3 on solid yeast extract-peptone-dextrose (YPD) medium. Fungal cell suspensions were prepared
4
5 by inoculating 10 mL medium with a single colony, and liquid cultures were incubated overnight
6
7 for 16 h at 30°C. A subculture was prepared by diluting the overnight culture into 10 mL fresh
8
9 YPD medium to an optical density (OD_{600}) of 0.1, where 1 OD corresponds to 2.4×10^7 colony
10
11 forming units/mL (CFU/mL). After 6 more hours of rotary shaking at 30 °C, after which all
12
13 strains were in exponential phase, 4.8×10^7 CFU were harvested and re-suspended in 150 μ L
14
15 sterile water (*i.e.*, 3.13×10^8 CFU/mL) and then uniformly spread on 6 cm diameter plates
16
17 containing 7 mL of solid YPD medium which had been pre-dried at 37 °C for 1 h. The
18
19 inoculating suspension was allowed to soak into the agar medium for 10 min, after which the
20
21 sensor array was exposed to the headspace, at room temperature, of the culture by replacing the
22
23 original petri dish lid with one containing the sensor array and sealing with parafilm. A control
24
25 with 150 μ L sterile water inoculation was performed in parallel in each trial.
26
27
28
29
30
31

32 For anti-fungal drug experiments, 20 μ L of stock drug solutions in dimethyl sulfoxide (DMSO)
33
34 were added to 130 μ L sterile water-suspended fungal cells. 20 μ L DMSO in 130 μ L sterile water
35
36 was used as control.
37
38
39

40 **2.2 Colorimetric sensor array and composite volatile response detection**

41
42
43

44 The disposable colorimetric sensor array was prepared by printing a 6x6 matrix of
45
46 nanoporous dyes onto polyvinylidene fluoride (PVDF) membrane. PVDF was chosen because it
47
48 is neutral, inert, and hydrophobic. The specific dyes used for this study is listed in Table S2. In
49
50 order to support the array in the head space of the culture and to easily conduct the experiments,
51
52 an engineered petri dish lid was designed. The colorimetric sensor array was attached to a plastic
53
54 stage via 3M double-sided tape (which showed no effect in controls), which allowed volatiles
55
56
57
58
59
60

1
2
3 diffuse and interact with all the dyes. The stage was then secured to the petri dish lid using
4
5 silicone oil (2×10^6 cSt). After the engineered lid was in place, the Petri dish was sealed with
6
7 parafilm and placed inverted on a commercially available scanner (Fig. S1) inside an incubator at
8
9 30 °C. Data was collected every 15 min using Epson Perfection V600 scanner.
10
11

12
13
14 Colour difference maps were generated by averaging the colour value changes of red, green
15
16 and blue (RGB), at each spot. The baseline values were taken 15 min after sealing the Petri dish.
17
18 Each strain has a unique colour difference map at each specific time point. Time response
19
20 profiles were obtained by plotting colour changes of all 108 channels (*i.e.*, ΔR , ΔG , ΔB values of
21
22 36 spots) over time (Fig. S3). The complete database is provided in Database S1.
23
24
25

26 27 **2.4 Linear Discriminant Analysis (LDA) and Tensor Discriminant Analysis (TDA)** 28

29
30 Linear discriminant analysis²⁸ was performed using a commercially available program,
31
32 SYSTAT13 (Systat Software Chicago, Illinois, USA, 2009). The data set consisted of 155 array
33
34 responses (*i.e.*, observations) at a single time (180 min). In the classification matrix (Table S3),
35
36 each observation is classified into the group where the value of its classification function is
37
38 largest. All 13 classes, including 12 strains and 1 background, were classified 100% correctly. A
39
40 Jackknifed classification (leave-one-out cross-validation) was used to test the predictability of
41
42 the sensor array: one observation is left out and the rest of the data are used as a training set to
43
44 generate the linear discriminant function, the model is then tested with the single left-out
45
46 observation, and the procedure is then iterated through all of the observations in turn. The
47
48 accuracy thus determined for the Jackknifed LDA prediction was 94%. The complete Jackknifed
49
50 classification matrix table is shown in Table S4.
51
52
53
54
55
56
57
58
59
60

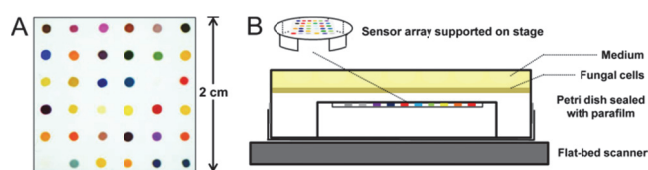
1
2
3 For our tensor discriminant analysis (TDA), we used the colour difference changes (ΔR ΔG
4 ΔB) from all 36 dye spots for 9 different times (from 120 min to 360 min in 30 min intervals).
5
6 TDA is a generalization of LDA to multiway arrays.²⁹⁻³¹ TDA constructs optimal linear
7
8 classifiers in a trimodal fashion, optimized separately for (1) the combination vector of dye spot,
9
10 (2) the effects of the three colour factors (ΔR ΔG ΔB) for each dye, and (3) the temporal
11
12 progression. The general strategy of the TDA algorithm in the colorimetric sensor array
13
14 classification can be clearly illustrated using the flow chart given below in Scheme S1.²⁹
15
16
17
18
19
20
21
22
23

24 **3. Results and Discussion**

25 **3.1 Colorimetric Sensor Arrays**

26
27
28
29
30
31 A colorimetric sensor array uses cross-reactive chemoresponsive colorants whose colour
32
33 changes reflect a diverse range of chemical interactions between the analytes and the colorants.
34
35 We have developed an optimized set of 36 dyes that yield an essentially universal chemical
36
37 sensor array.¹⁷ The dyes fall into four classes: (1) dyes containing metal ions (e.g.,
38
39 metalloporphyrins) that respond to Lewis basicity (that is, electron-pair donation, metal-ion
40
41 ligation), (2) pH indicators that respond to Brønsted acidity/basicity (that is, proton acidity and
42
43 hydrogen bonding), (3) dyes with large permanent dipoles (e.g., vapo chromic or solvatochromic
44
45 dyes) that respond to local polarity, and (4) metal salts that participate in redox and precipitatory
46
47 reactions. This colorimetric sensor array, therefore, is responsive to the chemical reactivity of
48
49 analytes, rather than to their effects on secondary physical properties (e.g., mass, conductivity,
50
51 adsorption, etc.). The specific dyes used for this study are given in Table S2.
52
53
54
55
56
57
58
59
60

1
2
3 We selected twelve clinically and commercially relevant fungal strains to test the CSA's
4 ability to differentiate strains based on their VOC profiles. These twelve strains (Table S1) were
5 grown on YPD agar (yeast extract, peptone, and dextrose), a commonly used rich growth
6 medium chosen because it accommodates a wide range of fungal strains. It is worth mentioning
7 that YPD medium (control, Fig. S3) also gives off volatiles. As a result, the signals obtained
8 from the CSA colour changes are from the combined volatiles from the YPD medium and from
9 the fungi.
10
11
12
13
14
15
16
17
18
19
20
21
22
23

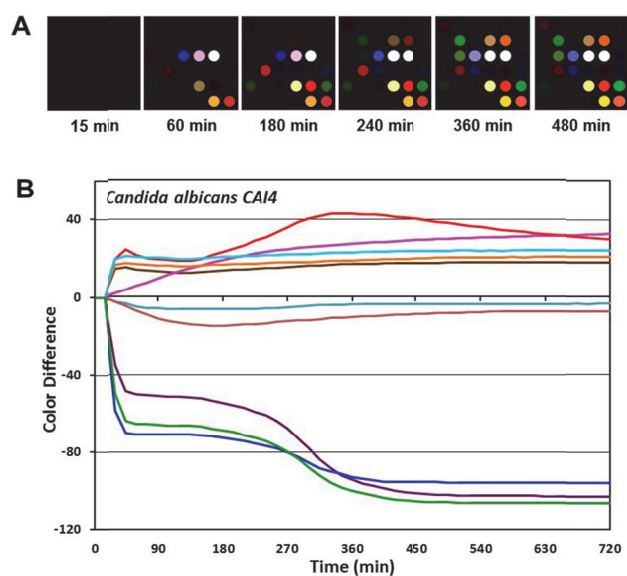


24
25
26
27
28
29
30
31 **Fig. 1** Schematic experimental apparatus. (A) An image of the CSA from a flat-bed scanner with
32 different responsive dyes printed on hydrophobic PVDF substrate. For a complete list of dyes
33 used in this research see Supporting Information. (B) Inverted Petri dish showing a colorimetric
34 sensor array supported in a plastic stage in the head gas volume. Fungal cells were uniformly
35 inoculated on YPD agar growth medium and the array digitally imaged with a flatbed scanner
36 inside an incubator at 30 °C. Colour changes were obtained as a function of time.
37
38
39
40
41
42
43
44
45

46 **3.2 Colour difference maps and time response profiles**

47
48
49 For analysis of the colorimetric sensor arrays, colour difference maps were generated from
50 the colour values (*i.e.*, red, green and blue (RGB) values) for each spot at any given time by
51 subtracting the baseline values of each spot taken at 15 min after the Petri dish was sealed.
52
53
54
55
56
57
58
59
60 Representative difference maps are given for *Candida albicans* (CAI-4) from 15 to 480 min are

1
2
3 given in Fig. 2A. At any given time, each of the 12 fungal strains shows a unique colour
4 difference map; for example, Fig. S2 shows the colour difference maps of the 12 strains after 180
5 min growth. The colour difference maps of all 12 strains are clearly differentiable by eye, even
6 before any statistical analysis. Qualitatively, one may easily differentiate among the three
7 *Candida albicans* strains, and identify *Debaryomyces hansenii*, which is often misdiagnosed as
8 *Candida guilliermondii*³².
9
10
11
12
13
14
15
16
17



38 **Fig. 2** Sensor array response to *Candida albicans* (CAI-4) out-gases. (A) Colour difference
39 maps (*i.e.*, ΔR , ΔG and ΔB of 36 sensor spots) at different time points were generated by
40 subtracting the RGB values from baseline at 15 minutes after sealing of Petri dish. For
41 visualization in the colour difference maps, four bit colour was expanded to 8 bit colour (*i.e.*, the
42 RGB values of 4-19 were expanded to 0-255). (B) Temporal profile from the 10 most responsive
43 channels vs. time.
44
45
46
47
48
49
50
51
52
53
54

55 Time response profiles were obtained by plotting the colour changes of the individual
56 channels (*i.e.*, ΔR , ΔG , ΔB values for 36 spots) vs. time. For clarity of presentation, only the ten
57
58
59
60

1
2
3 most responsive channels are shown in Fig. 2B, again for *C. albicans* as an example. The time
4 response profiles for all 12 strains of fungi are provided as Fig. S3. The differences in the time
5 response provides for each of the fungal strains serve as fingerprints that allow one both to
6 qualitatively differentiate and identify strains even by the naked eye and to provide a quantitative
7 pattern analysis.
8
9

10
11
12
13
14
15
16 The time response profiles for different fungal strains vary both in the intensities of the
17 colour changes and in the times at which such response begin to occur. For example, thiols and
18 sulfides are common metabolites among fungi,³³ and the sensor spot that are most responsive to
19 thiols and sulfides (*i.e.*, the blue, green, and purple lines in Figure 2B and Figure S3) do indeed
20 undergo large colour changes. The timings of these colour changes, however, are strain specific:
21 rapid changes occur for *C. albicans* (CAI-4) (even after just 15 min), whereas the changes begin
22 to occur only after 180 min for *C. keyfr*, 450 min for *C. stellatoidea*, and not at all with *D.*
23 *hansenii*. This thiol and sulfide responding spot has a dye formulation containing $\text{Pb}(\text{O}_2\text{CCH}_3)_2$
24 (Table S2).
25
26
27
28
29
30
31
32
33
34
35
36
37

38 **3.4 Pattern Recognition and Statistical Analysis**

39

40
41
42 To provide a statistically meaningful analysis, we utilized a standard chemometric approach,
43 hierarchical cluster analysis (HCA),²⁸ to discriminate the VOC temporal profiles among the 12
44 strains and to demonstrate excellent reproducibility among replicates. HCA is a model-free
45 clustering analysis that generates a dendrogram based on the Euclidean distances between the
46 difference maps of each trial using all 108 dimensions. No mis-clusterings were observed for
47 data from 155 trials after 180 min growth (Fig. 3A), which demonstrates that the method is
48 reproducible and differentiates among different strains of fungi. It is worth noting that the
49
50
51
52
53
54
55
56
57
58
59
60

clustering is not directly related to fungal phylogenetic classifications. This is not surprising as our methodology detects metabolic byproducts and is only indirectly responsive to genomic sequence: we are probing the metabolomics of the microorganisms, not their genomes.

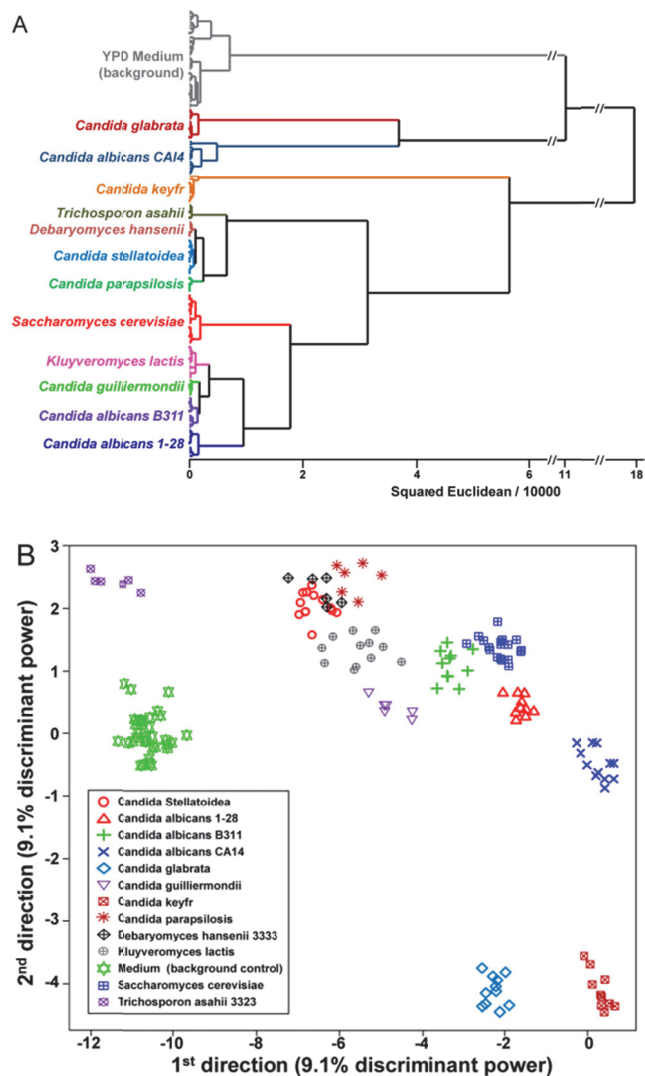


Fig. 3 Classification analysis. (A) Hierarchical cluster analysis dendrogram (using Ward's method) of 12 fungal strains and YPD medium background at 180 min with 2.4×10^7 colony forming units of inoculation; no errors in clustering were observed among a total of 155 trials. (B) Scatter plot of the first two directions from the tensor discriminant analysis. Surprising good discrimination of the fungal strains is achieved even with only two TDA directions, which

1
2
3 account for only 18.2% of the total discriminant power. The accuracy of classification using
4
5 TDA maximizes at 98.1% using an optimal 10 dimensions.
6
7
8
9
10

11
12 To provide a quantitative evaluation of the accuracy of classification of the fungal strains by
13 our colorimetric sensor arrays, we first completed a standard linear discriminant analysis (LDA).
14 LDA of the array response (*i.e.*, the RGB colour changes of each sensor spot) at 180 min gave a
15 classification matrix with no errors (Table S3). To quantitatively test the prediction accuracy of a
16 new unknown input using LDA, a standard Jackknifed analysis was performed (leaving out one
17 observation at a time and permuting through the full dataset), giving a prediction accuracy of
18 94% (Table S4). Data from these colorimetric sensor arrays have an exceptionally high
19 dimensionality, and LDA does not provide optimal classification with such data due to the “curse
20 of dimensionality” (*i.e.*, the difficulties that a large number of dimensions can create for function
21 approximation, model fitting, information extraction, as well as computation).³⁴
22
23
24
25
26
27
28
29
30
31
32
33
34
35
36

37 Tensor discriminant analysis (TDA) is an array generalization of LDA better able to take
38 advantage of high dimensionality.^{30, 31} More precisely, tensor discriminant analysis is used to
39 classify multi-way array measurements (*i.e.*, “tensor measurements”), rather than one-way vector
40 measurements. The data collected using colorimetric sensor arrays can be viewed as a 3-way
41 tensor with the first mode corresponding to choice of the dye, the second mode corresponding to
42 the effects of the colour changes (*i.e.*, ΔR , ΔG , ΔB), and the third mode corresponding to the
43 time progression.²⁹ The general strategy of tensor discriminant analysis is to find orthogonal
44 linear classifiers so as to maximize the ratio of between-class variation to within-class variation
45 (*i.e.*, to maximize discrimination among classes). Those orthogonal linear classifiers are
46
47
48
49
50
51
52
53
54
55
56
57
58
59
60

1
2
3 essentially linear combinations of the three-way interactions of (1) the effects of the dye spot
4 choice, (2) the three colour changes of each spot (*i.e.*, ΔR , ΔG , ΔB), and (3) the temporal
5 evolution.
6
7
8
9

10
11 Tensor discriminant analysis can greatly improve the sensitivity, specificity, and
12 computational efficiency of discriminant analysis method.²⁹⁻³¹ LDA and most other existing
13 classification methods largely ignore the array structure of the colorimetric sensor array data: the
14 three colour changes for each spot are not fully independent dimensions compared to the three
15 colour changes of the other spots. For our array data over time, LDA would simply vectorize
16 each 3-way observation into a vector with 972 dimensions ($36 \times 3 \times 9$, *i.e.*, where 36 dyes \times 3
17 colour factors (ΔR ΔG ΔB) \times 9 time points (120 min to 360 min in 30 min intervals)) and find
18 classifiers using 972 parameters. In contrast, TDA constructs the optimal linear classifiers and
19 estimates them in a trimodal tensor (separating spot choice, colour, and time). By separating
20 these three classes of effects, we can (1) keep the original design information and avoid
21 interpretation difficulties, (2) substantially limit the effective dimensionality (we only need 48
22 parameters (*i.e.*, $36+3+9$) for TDA, rather than 972 parameters in LDA or PCA), and (3) improve
23 prediction accuracy.
24
25
26
27
28
29
30
31
32
33
34
35
36
37
38
39
40
41
42

43 As a result, the directions created in TDA are not obscured by the noise present in the very
44 large number of additional dimensions in LDA or PCA. As a consequence, excellent
45 discrimination of the fungal strains is achieved even with only two TDA directions, which
46 account for only 18.2% of the total discriminant power (as defined by the ratio of the between-
47 group variation to the within-group variation), as seen in Figure 3B. The prediction accuracy of
48 TDA was assessed quantitatively by using a Jackknifed classification (leave-one-out cross-
49 validation using the rest of the data as a training set and permuting through the full dataset). The
50
51
52
53
54
55
56
57
58
59
60

1
2
3 prediction accuracy of the tensor discriminant analysis reaches a maximum of 98.1% using an
4
5 optimal 10 dimensions (Fig. S4, based on 155 trials).
6
7
8
9
10

11 12 **3.5 Limit of Detection** 13

14
15
16 The limit of detection (LOD) at a given time may be defined as the smallest number of viable
17
18 fungal cells in the initial inoculum that will give a response from a single channel that is larger
19
20 than three times the noise at that given time. A more quantitative measure of the LOD at 720 min
21
22 can be approximated as $3[I]\sigma/C_{\max}$ where $[I]$ is the initial inoculum concentration, σ is the
23
24 standard deviation of the channel with the largest net colour response at 720 min, and C_{\max} is that
25
26 largest net colour response. Time response profiles of the 10 most responsive channels of array
27
28 response to *Candida albicans* (CAI-4) is shown in Figure 4. We can interpolate the LOD from
29
30 the three lowest initial inocula (Fig. S5), and calculate the LOD after 720 min. to be 2×10^4 CFU
31
32 for the initial inoculum. One may also define a *time to detection* as the time at which the
33
34 response of a single channel is larger than three times the noise. Not surprisingly, there is a
35
36 roughly linear correlation between the time to detection vs. the log of the initial inoculum (Fig.
37
38 S6); for example, with an initial inoculum of 10^6 CFU, the time to detection is ~ 400 min.
39
40
41
42
43
44
45
46
47
48
49
50
51
52
53
54
55
56
57
58
59
60

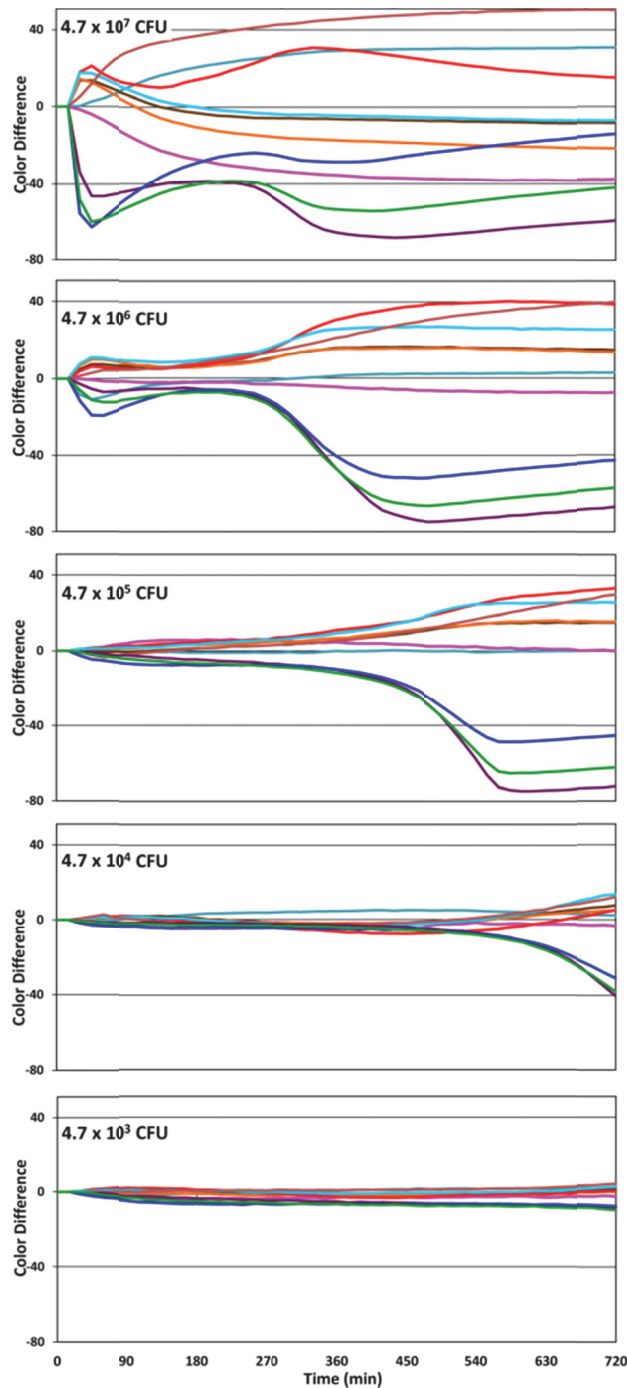


Fig. 4 Time response profiles of the 10 most responsive channels of array response to *Candida albicans* (CAI-4) after subtraction of the YPD growth medium background. As the initial inoculum is decreased, the time response profiles decrease in intensity. At 720 min, the LOD is approximately 2×10^4 CFU.

3.6 Effects of Fungicides on Metabolic Patterns

Although chemical profiling at a single time point can be achieved by methods such as GC-MS, monitoring the changing VOC profile continuously during culture growth is challenging. Using this colorimetric sensor array, however, one can monitor cell growth conditions continuously and inexpensively. It is well established that there are changes of metabolic states in response to fungicides^{35,36}, and we should expect that the VOCs produced by the fungi should therefore change under drug induced stress. In this manner, the colorimetric sensor array can be used to monitor changes in fungal metabolic states or in response to fungicides during cell growth.

Indeed, the array response (as measured by the total change in the Euclidian distance (ΔED) of all 108 colour channels) of *C. albicans* (CAI-4) is substantially affected by the presence of various concentrations of clotrimazole or miconazole (Fig. 5A). The colour difference maps (Fig. 5B) demonstrate the shut-down of VOC production at high concentrations of anti-fungal drugs: volatiles are no longer being released (and the ΔED of the sensor array no longer changes) after roughly 180 min, for clotrimazole at $>400 \mu\text{g/mL}$ and for miconazole at $>0.5 \mu\text{g/mL}$, which represent the minimum inhibitory concentrations of two drugs. At lower concentrations, the volatile metabolites are clearly changed, relative to untreated fungi, which can lead to either greater or diminished sensor array response (Fig. 5B). While the colorimetric sensor array does not provide a direct indication of what the changes in the VOCs may be (*i.e.*, the component by component analysis provided by GC-MS, for example), it does yield a rapid and simple indication that significant metabolic changes are occurring. This could prove useful for rapid parallel screening of fungicidal effectiveness.

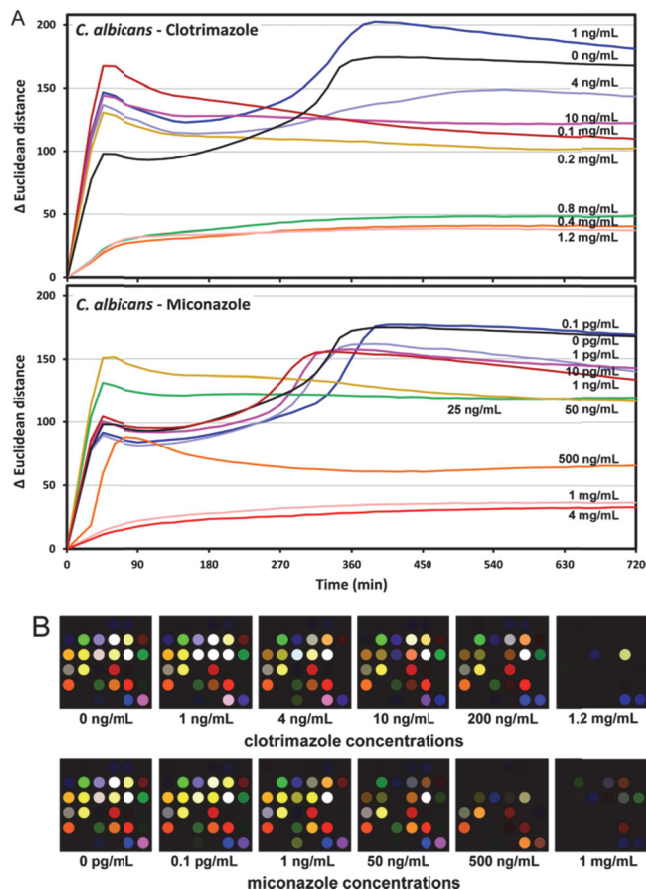


Fig. 5 Sensor array response to fungal volatiles under the influence of anti-fungal drugs. (A) Total array response (change in Euclidean distance after subtraction of background) under the influence of fungicidal drugs. Significant changes in array response are observed vs. clotrimazole or miconazole concentrations. (B) Colour difference maps vs. YPD growth medium control after 400 min as a function of fungicide concentration. Changes in the array response patterns appear to occur at ≥ 10 ng/mL clotrimazole and at ≥ 1 ng/mL for miconazole, which are presumably due to changes of metabolic states under the stress of the anti-fungal drug environment. The complete shutdown of volatile metabolites occurs at >400 $\mu\text{g/mL}$ clotrimazole and at >0.5 $\mu\text{g/mL}$ miconazole.

4. Conclusions

In summary, we have used an optoelectronic nose to detect fungal VOCs and generate unique metabolic patterns that differentiate among twelve different fungal strains with high accuracy. The sensor array is also able to observe metabolic changes in growth patterns upon the addition of fungicides, which provides a facile screening tool for determining fungicide efficacy in real time.

Acknowledgments

This work was supported through NIH GEI award U01ES016011. We thank Professor Lois L. Hoyer for generously providing fungal strains. We thank Jacqueline M. Rankin and John R.G. Sander for helpful suggestions and advice. KSS has financial interests in iSense LLC, which is commercializing applications of colorimetric sensor arrays. No funding from iSense was involved in this research.

References

1. G. D. Brown, D. W. Denning, N. A. R. Gow, S. M. Levitz, M. G. Netea and T. C. White, *Science Translational Medicine*, 2012, **4**, 1-9.
2. G. D. Brown, D. W. Denning and S. M. Levitz, *Science*, 2012, **336**, 647-647.
3. M. Nucci and K. A. Marr, *Clin. Infect. Dis.*, 2005, **41**, 521-526.
4. P. R. Murray and H. Masur, *Critical care medicine*, 2012, **40**, 3277-3282.
5. B. M. Kuehn, *JAMA-J. Am. Med. Assoc.*, 2013, **309**, 219-221.
6. J. S. Klutts and B. Robinson-Dunn, *J. Clin. Microbiol.*, 2011, **49**, S39-S42.
7. S. F. Yeo and B. Wong, *Clin. Microbiol. Rev.*, 2002, **15**, 465-484.
8. S. U. Morath, R. Hung and J. W. Bennett, *Fungal Biol. Rev.*, 2012, **26**, 73-83.
9. N. Sahgal, B. Monk, M. Wasil and N. Magan, *Br. J. Dermatol.*, 2006, **155**, 1209-1216.
10. J. M. Scotter, V. S. Langford, P. F. Wilson, M. J. McEwan and S. T. Chambers, *J. Microbiol. Methods*, 2005, **63**, 127-134.
11. N. Sahgal and N. Magan, *Sensors Actuators B: Chem.*, 2008, **131**, 117-120.
12. K. Naraghi, N. Sahgal, B. Adriaans, H. Barr and N. Magan, *Sensors Actuators B: Chem.*, 2010, **146**, 521-526.
13. N. P. Pont, C. A. Kendall and N. Magan, *Mycopathologia*, 2012, **173**, 93-101.
14. F. Rock, N. Barsan and U. Weimar, *Chem. Rev.*, 2008, **108**, 705-725.
15. N. A. Rakow and K. S. Suslick, *Nature*, 2000, **406**, 710-713.
16. K. S. Suslick, *Current Opinion Chem. Biol.*, 2012, **16**, 557-563.
17. S. H. Lim, L. Feng, J. W. Kemling, C. J. Musto and K. S. Suslick, *Nat. Chem.*, 2009, **1**, 562-567.
18. M. C. Janzen, J. B. Ponder, D. P. Bailey, C. K. Ingison and K. S. Suslick, *Anal. Chem.*, 2006, **78**, 3591-3600.
19. K. S. Suslick, D. P. Bailey, C. K. Ingison, M. Janzen, M. E. Kosal, W. B. McNamara III, N. A. Rakow, A. Sen, J. J. Weaver, J. B. Wilson, C. Zhang and S. Nakagaki, *Quim. Nova*, 2007, **30**, 677-681.
20. L. Feng, C. J. Musto, J. W. Kemling, S. H. Lim, W. Zhong and K. S. Suslick, *Anal. Chem.*, 2010, **82**, 9433-9440.
21. L. Feng, C. J. Musto, J. W. Kemling, S. H. Lim and K. S. Suslick, *Chem. Commun.*, 2010, **46**, 2037-2039.
22. H. Lin and K. S. Suslick, *J. Am. Chem. Soc.*, 2010, **132**, 15519-15521.
23. B. A. Suslick, L. Feng and K. S. Suslick, *Anal. Chem.*, 2010, **82**, 2067-2073.
24. C. Zhang, D. P. Bailey and K. S. Suslick, *J. Agric. Food Chem.*, 2006, **54**, 4925-4931.
25. C. Zhang and K. S. Suslick, *J. Agric. Food Chem.*, 2007, **55**, 237-242.
26. J. R. Carey, K. S. Suslick, K. I. Hulkower, J. A. Imlay, K. R. Imlay, C. K. Ingison, J. B. Ponder, A. Sen and A. E. Wittrig, *J. Am. Chem. Soc.*, 2011, **133**, 7571-7576.
27. P. J. Mazzone, X. F. Wang, Y. M. Xu, T. Mekhail, M. C. Beukemann, J. Na, J. W. Kemling, K. S. Suslick and M. Sasidhar, *Journal of Thoracic Oncology*, 2012, **7**, 137-142.
28. S. J. Haswell, *Practical guide to chemometrics*, CRC Press, 1992.
29. W. Zhong and K. S. Suslick, *Technometrics*, 2013, **55**, in press. http://publish.illinois.edu/wenxuan/files/2012/2012/matrix_clust.pdf
30. B. Li, K. M.K. and N. Altman, *Ann. Statist.*, 2010, **38**, 1094-1121.
31. P. Zeng and W. Zhong, *Dimension reduction for tensor classification*, New York, 2013.

- 1
- 2
- 3
- 4 32. M. Desnos-Ollivier, M. Ragon, V. Robert, D. Raoux, J.-C. Gantier and F. Dromer, *J. Clin. Microbiol.*, 2008, **46**, 3237-3242.
- 5
- 6 33. G. L. Newton, K. Arnold, M. S. Price, C. Sherrill, S. B. Delcardayre, Y. Aharonowitz, G. Cohen, J. Davies, R. C. Fahey and C. Davis, *J. Bacteriol.*, 1996, **178**, 1990-1995.
- 7
- 8 34. D. L. Donoho, *AMS Math Challenges Lecture*, 2000, 1-32 www-stat.stanford.edu/~donoho/Lectures/AMS2000/Curses.pdf.
- 9
- 10 35. P. Belenky, D. Camacho and J. J. Collins, *Cell Reports*, 2013, **3**, 350-358.
- 11 36. R. D. Cannon, E. Lamping, A. R. Holmes, K. Niimi, K. Tanabe, M. Niimi and B. C. Monk, *Microbiology*, 2007, **153**, 3211-3217.
- 12
- 13
- 14
- 15
- 16
- 17
- 18
- 19
- 20
- 21
- 22
- 23
- 24
- 25
- 26
- 27
- 28
- 29
- 30
- 31
- 32
- 33
- 34
- 35
- 36
- 37
- 38
- 39
- 40
- 41
- 42
- 43
- 44
- 45
- 46
- 47
- 48
- 49
- 50
- 51
- 52
- 53
- 54
- 55
- 56
- 57
- 58
- 59
- 60